

基于轴手性配体的两个镧系金属配合物的合成、表征及其荧光性质

吉 沁 陈立庄*

(江苏科技大学环境与化学工程学院, 镇江 212003)

摘要: 通过水热法, 合成了 2 个基于轴手性配体 2,2'-dinitro-4,4'-biphenyldicarboxylic acid (H_2nbpdc) 的配位聚合物 $[La(nbpdc)(phen)(FA)]_n$ (**1**), $[Eu(nbpdc)(phen)(FA)]_n$ (**2**) ($phen$ =菲咯啉, FA =甲酸根), 并且对 2 个化合物进行了红外、单晶 X 射线衍射、热重、荧光、CD 谱及介电性质的研究。晶体结构测试表明, 2 个化合物结晶在正交晶系 $P2_12_12_1$ 手性空间群, 且具有相同的三维拓扑结构。荧光性质测定表明化合物 **1** 和 **2** 分别在 606 和 615.5 nm 处有强的发射光谱。与此同时, 固体 CD 谱测试进一步证实 2 个化合物具有手性。

关键词: 配位聚合物; 水热反应; 荧光; 手性

中图分类号: O614.33^{†1}; O614.33^{†8}

文献标识码: A

文章编号: 1001-4861(2017)05-0874-07

DOI: 10.11862/CJIC.2017.099

Syntheses, Characterization and Fluorescence Properties Analysis of Two Lanthanide Coordination Polymers Based on Axial Chirality Ligand 2,2'-Dinitro-4,4'-biphenyldicarboxylic Acid

JI Qin CHEN Li-Zhuang*

(School of Environmental and Chemical Engineering, Jiangsu University of Science and Technology, Zhenjiang, Jiangsu 212003, China)

Abstract: Two lanthanide coordination polymers, $La(nbpdc)(phen)(FA)$ (**1**), $Eu(nbpdc)(phen)(FA)$ (**2**) (FA =formic acid ion) based on bridging ligand 2,2'-dinitro-4,4'-biphenyldicarboxylic acid (H_2nbpdc) and 1,10-Phenanthroline monohydrate ($phen$), have been synthesized by the hydrothermal method and characterized by IR, single-crystal X-ray structure analysis, thermogravimetric analysis, luminescent properties, circular dichroism (CD) analysis and dielectric properties. Complexes **1** and **2** exhibited a rare three-interlode 3D structure with the same topology structure of $(4^4 \cdot 6^2)$. In addition, the two complexes exhibit fluorescent emissions in the solid state at room temperature. Fluorescent analysis of complexes **1** and **2** showed an intense emission band at 606 nm (λ_{ex} =495 nm) and 615.5 nm (λ_{ex} =395.5 nm), respectively. Moreover, the circular dichroism analysis of complexes **1** and **2** was measured with chirality. CCDC: 1504875, **1**; 1504877, **2**.

Keywords: coordination polymer; hydrothermal condition; fluorescence; chirality

收稿日期: 2016-11-14。收修改稿日期: 2017-03-09。

国家自然科学基金(No.21671084)、江苏省自然科学基金(No.BK20131244)、江苏省“六大人才高峰”项目(No.2014-XCL-008)、江苏省青蓝工程项目、江苏省高校研究生实践创新计划项目(No.KYLX16-0508)和江苏教育厅基金(No.16KJB430011)资助。

*通信联系人。E-mail: clz1977@sina.com

Coordination polymers have received attention because of the intriguing structures and potential applications in magnetism, catalysis, luminescence, conductivity, sensors, porosity, nonlinear optics, *etc*^[1-18]. Luminescent lanthanide complexes have been extensively studied due to extremely narrow emission bands, large Stokes shift, long luminescence decay times, and no theoretical cap on quantum efficiency; particularly, europium, terbium, samarium, and dysprosium have interesting luminescent properties, such as red emission for Eu(III) ion. They are very attractive for applications in light-emitting diodes^[19], laser materials^[20], and as probes and labels in a variety of biological and chemical applications^[21-22]. Luminescent intensities of lanthanide complexes are dependent on the ligands. In our continuing effort in this field^[23-24], we chose ligand 2,2'-dinitro-4,4'-biphenyldicarboxylic acid (H₂nbpdc) as an organic building block in an attempt to construct coordination polymers with new structural features. In addition, the two benzoate moieties in nbpdc twist freely due to two nitro groups, thus bringing about an organic building block which is geometrically different from the mother ligand and hence may lead to different topologies. Moreover, nbpdc ligand may induce cluster aggregation and link the clusters into extended networks. However, to the best of our knowledge, frameworks based on ligand nbpdc have rarely been studied^[25]. Herein, we report the synthesis, crystal structure, and luminescent properties of two lanthanide(III) complexes.

1 Experimental

1.1 Materials and physical measurements

All of the chemicals and solvents except for nbpdc ligand in this study obtained from Shanghai Jingchun Scientific Company were of reagent grade and used without any further purification. The nbpdc ligand was prepared by the method reported previously^[26]. Infrared spectra were recorded on a SHIMADZU IR prestige-21 FTIR-8400S spectrometer in the spectral range of 4000~500 cm⁻¹ with samples in the form of potassium bromide pellets. Elemental analyses were taken on a Perkin-Elmer 240C elemental analyzer.

The solid-state fluorescent spectra were recorded by Spectrofluorometer FS5 at room temperature. Thermogravimetric analyses (TGA) were conducted on a NETZSCH TG 209 F3 thermo gravimeter with the heating rate of 10 K·min⁻¹ in a N₂ atmosphere. The chirality of complexes was characterized by JASCO J-1500 circular dichroism.

1.2 Preparation of complex 1

H₂nbpdc (0.1 mmol, 0.033 0 g), phen (0.1 mmol, 0.019 8 g) and La(NO₃)₃ (0.1 mmol, 0.043 3 g) were placed in a 25 mL Teflon-lined stainless-steel vessel. After the addition of water (1.5 mL) and DMF (1.5 mL), the solution was heated to 125 °C for three days. Afterwards, the reaction system was slowly cooled down (a descent rate of 5 °C·h⁻¹) to room temperature. Colorless transparent bulk crystals were obtained, washed with distilled water, and dried in air. Yield: 64% (based on nbpdc). Anal. Calcd.(%) for C₂₇H₁₄N₄O₁₀La: C, 46.73; H, 2.01; N, 8.08. Found (%): C, 45.47; H, 1.96; N, 7.39. IR data (KBr pellet, cm⁻¹) (Fig.S1): 3 402 (w), 3 090 (w), 2 922 (w), 2 838 (w), 1 599(s), 1 515(m), 1 396(s), 1 335(s), 1 094(w), 913(w), 842 (m), 770(s), 710(m), 517(w).

1.3 Preparation of complex 2

The synthesis of **2** was similar with **1** except that Eu(NO₃)₃ (0.1 mmol, 0.044 6 g) was used instead of La(NO₃)₃. Colorless block crystals were obtained in 52% yield. Anal. Calcd.(%) for C₂₇H₁₅N₄O₁₀Eu: C, 45.80; H, 2.12; N, 7.92. Found (%): C, 44.93; H, 2.03; N, 6.46. IR data (KBr pellet, cm⁻¹) (Fig.S2): 3 402(s), 3 086(m), 2 948(w), 2 855(w), 1 652(w), 1 596(w), 1 523 (s), 1 403(s), 1 338(m), 1 078(m), 995(w), 912(m), 839 (s), 773(s), 719(s), 624(m).

1.4 Single-crystal X-ray diffraction

Single crystals of **1** and **2** with appropriate dimensions (0.26 mm×0.30 mm×0.24 mm for **1**, 0.30 mm×0.30 mm×0.20 mm for **2**) were selected for data collection on a Rigaku SCXmini diffractometer equipped with a graphite-monochromated Mo K α radiation (λ =0.071 073 nm), using an ω scan mode at 296 K. The absorption correction was carried out by a multi-scan method. The structures were solved by direct methods with SHELXS-97 and refined by full-matrix least-

squares on F^2 with SHELXL-97^[27-28]. While H atoms were located in calculated positions and refined using a riding model, which were found by electron cloud density. Some disordered solvent molecules were treated by SQUEEZE^[29] process. Topology information for complexes **1**~**2** was obtained using TOPOS 4.0^[30]. All non-hydrogen atoms were refined with anisotropic thermal parameters. All hydrogen atoms attached to C,

N and O atoms were added theoretically and refined with a riding model and fixed isotropic thermal parameters. Detailed data collection and refinement of complexes **1** and **2** are summarized in Table 1, and the selected bond distances and bond angles of **1** and **2** are listed in Table 2 and 3, respectively.

CCDC: 1504875, **1**; 1504877, **2**.

Table 1 Data collection and processing parameters for **1** and **2**

	1	2
Formula	C ₂₇ H ₁₄ N ₄ O ₁₀ La	C ₂₇ H ₁₅ N ₄ O ₁₀ Eu
Formula weight	693.33	707.39
Crystal system	Orthorhombic	Orthorhombic
Space group	<i>P</i> 2 ₁ 2 ₁ 2 ₁	<i>P</i> 2 ₁ 2 ₁ 2 ₁
<i>a</i> / nm	0.855 20(9)	0.848 78(5)
<i>b</i> / nm	1.096 95(10)	1.086 70(5)
<i>c</i> / nm	2.727 4(2)	2.690 14(13)
<i>V</i> / nm ³	2.558 7(4)	2.481 3(2)
<i>Z</i>	4	4
<i>D_c</i> / (g·cm ⁻³)	1.800	1.894
μ / mm ⁻¹	1.739	2.599
<i>R</i> ₁ , <i>wR</i> ₂ (<i>I</i> > 2 σ (<i>I</i>))	0.024 3, 0.056 7	0.028 3, 0.070 7
<i>R</i> ₁ , <i>wR</i> ₂ (all data)	0.030 3, 0.075 6	0.030 4, 0.084 2
Flack	0.000(15)	0.005(13)

Table 2 Selected bond lengths (nm) and bond angles (°) of **1**

La(1)-N(1)	0.275 7(3)	La(1)-O(2)	0.245 7(3)	La(1)-O(4)	0.253 9(3)
La(1)-O(4)	0.281 2(3)	La(1)-O(6)	0.247 6(3)	La(1)-O(7)	0.250 0(3)
La(1)-O(1)	0.248 7(3)	La(1)-N(3)	0.276 7(4)	La(1)-C(4)	0.302 9(4)
La(1)-O(3)	0.255 1(3)				
N(1)-La(1)-O(4)	110.65(10)	N(1)-La(1)-N(3)	59.43(11)	N(1)-La(1)-C(4)	91.16(11)
O(2)-La(1)-N(1)	141.66(10)	O(2)-La(1)-O(4)	71.26(9)	O(2)-La(1)-O(4)	65.77(9)
O(2)-La(1)-O(6)	74.90(10)	O(2)-La(1)-O(7)	88.94(10)	O(2)-La(1)-O(1)	133.84(10)
O(2)-La(1)-N(3)	146.21(11)	O(2)-La(1)-C(4)	71.67(10)	O(2)-La(1)-O(3)	77.85(10)
O(4)-La(1)-N(1)	119.20(10)	O(4)-La(1)-O(4)	129.72(3)	O(4)-La(1)-N(3)	74.95(10)
O(4)-La(1)-C(4)	142.92(10)	O(4)-La(1)-C(4)	24.64(9)	O(4)-La(1)-O(3)	141.96(10)
O(6)-La(1)-N(1)	72.70(10)	O(6)-La(1)-O(4)	114.40(9)	O(6)-La(1)-O(4)	76.51(10)
O(6)-La(1)-O(7)	147.86(10)	O(6)-La(1)-O(1)	137.32(10)	O(6)-La(1)-N(3)	97.85(11)
O(6)-La(1)-C(4)	94.86(10)	O(6)-La(1)-O(3)	74.41(10)	O(7)-La(1)-N(1)	129.22(10)
O(7)-La(1)-O(4)	71.99(10)	O(7)-La(1)-O(4)	82.18(9)	O(7)-La(1)-N(3)	80.18(11)
O(7)-La(1)-C(4)	106.35(10)	O(7)-La(1)-O(3)	129.78(10)	O(1)-La(1)-N(1)	66.90(10)
O(1)-La(1)-O(4)	69.75(9)	O(1)-La(1)-O(4)	135.96(10)	O(1)-La(1)-O(7)	73.22(10)
O(1)-La(1)-N(3)	73.24(11)	O(1)-La(1)-C(4)	73.24(10)	O(1)-La(1)-O(3)	81.83(10)
N(3)-La(1)-O(4)	142.22(10)	N(3)-La(1)-C(4)	142.08(11)	O(3)-La(1)-N(1)	74.19(10)
O(3)-La(1)-O(4)	48.11(9)	O(3)-La(1)-N(3)	132.86(10)	O(3)-La(1)-C(4)	23.55(10)

Table 3 Selected bond lengths (nm) and bond angles ($^{\circ}$) of **2**

Eu(1)-O(2)	0.236 9(4)	Eu(1)-O(7)	0.238 1(3)	Eu(1)-O(1)	0.238 4(3)
Eu(1)-O(8)	0.239 8(4)	Eu(1)-O(10)	0.242 0(3)	Eu(1)-O(9)	0.242 3(3)
Eu(1)-N(2)	0.266 5(4)	Eu(1)-N(1)	0.268 0(5)	Eu(1)-O(10)	0.286 2(3)
O(2)-Eu(1)-O(7)	75.72(13)	O(2)-Eu(1)-O(1)	132.07(12)	O(7)-Eu(1)-O(1)	137.28(14)
O(2)-Eu(1)-O(8)	86.29(13)	O(7)-Eu(1)-O(8)	147.85(13)	O(1)-Eu(1)-O(8)	74.03(13)
O(2)-Eu(1)-O(10)	71.93(12)	O(7)-Eu(1)-O(10)	75.94(13)	O(1)-Eu(1)-O(10)	137.13(13)
O(8)-Eu(1)-O(10)	73.20(12)	O(2)-Eu(1)-O(9)	77.57(13)	O(7)-Eu(1)-O(9)	75.38(11)
O(1)-Eu(1)-O(9)	80.32(12)	O(8)-Eu(1)-O(9)	126.85(12)	O(10)-Eu(1)-O(9)	142.24(12)
O(2)-Eu(1)-N(2)	146.06(13)	O(7)-Eu(1)-N(2)	98.23(13)	O(1)-Eu(1)-N(2)	74.52(12)
O(8)-Eu(1)-N(2)	81.94(15)	O(10)-Eu(1)-N(2)	74.20(13)	O(9)-Eu(1)-N(2)	134.03(14)
O(1)-Eu(1)-N(2)	74.52(12)	O(1)-Eu(1)-N(1)	74.52(12)	O(1)-Eu(1)-N(1)	74.52(12)
O(2)-Eu(1)-N(1)	141.14(13)	O(7)-Eu(1)-N(1)	72.13(13)	O(1)-Eu(1)-N(1)	67.55(12)
O(8)-Eu(1)-N(1)	132.10(13)	O(10)-Eu(1)-N(1)	119.25(12)	O(9)-Eu(1)-N(1)	73.69(13)
N(2)-Eu(1)-N(1)	61.34(14)	O(2)-Eu(1)-O(10)	65.16(11)	O(7)-Eu(1)-O(10)	115.27(11)
O(1)-Eu(1)-O(10)	68.37(11)	O(8)-Eu(1)-O(10)	79.17(12)	O(10)-Eu(1)-O(10)	129.82(4)
O(9)-Eu(1)-O(10)	48.02(11)	N(2)-Eu(1)-O(10)	141.70(12)	N(1)-Eu(1)-O(10)	110.44(12)

1.5 Dielectric measurements

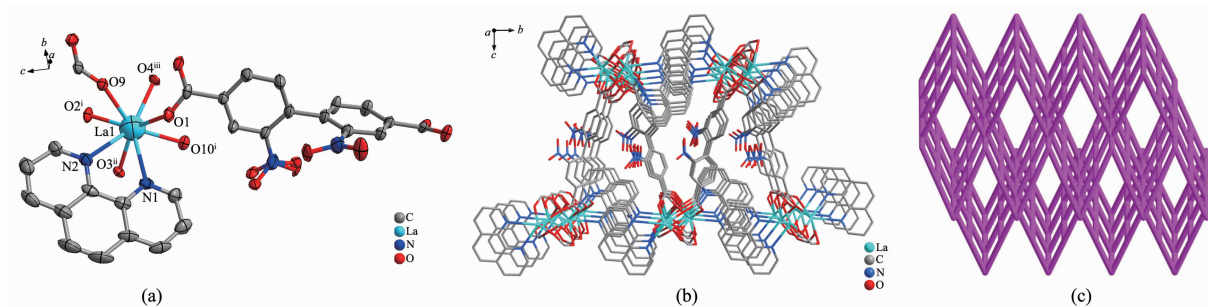
The temperature dependences of the dielectric constants of two complexes were measured on the Tonghui TH2828A analyzer in the temperature ranges of 120~290 K and 150~230 K, respectively, within the frequency range of 500 Hz to 1 MHz at the AC voltage of 1 V. Crystals of the two compounds with appropriate dimensions were prepared with silver-conductive glue and used for dielectric studies.

2 Results and discussion

2.1 Crystal structures of **1** and **2**

Single-crystal X-ray diffraction reveals that complexes **1** and **2** crystallize in the orthorhombic system, space group $P2_12_12_1$ and displays a 3D coor-

dination framework. Complexes **1** and **2** are isostructural, so the crystal structure of **1** is described in detail. As shown in Fig.1a, the asymmetric unit of crystal **1** contains one La(III) ion, one nbpdc ligand, one phen and one formic acid ion (FA). Besides, the La(III) is in a slightly distorted dodecahedral environment. Moreover, it is interesting that only ligand nbpdc coordinates metal La(III) ion as a two-dimensional network that gradually forms a three-dimensional structure by coordinating phen and La(III) ions (Fig.1b). To get a better insight into the structure of complex **1**, topological analysis was conducted. Each 2-connected bridging nbpdc ligand can be regarded as a linear linker. Each phen ligand can also be treated as a 2-connector and each La(III) ion can be regarded as 8-



Symmetry codes: ⁱ -0.5+x, 2.5-y, 2-z; ⁱⁱ 1.5-x, 2-y, 0.5+z; ⁱⁱⁱ 2-x, 0.5+y, 1.5-z

Fig.1 (a) View of the coordination environment of La(III) in complex **1** with displacement ellipsoids drawn at the 50% probability level; (b) Three-dimensional structure of complex **1**; (c) Topological analysis of complex **1**

connected node since it links four nbpd, one phen and two formic acid ions. Thus, the simplified overall structure of **1** is 4-connected uninodal net with stoichiometry (4-c), as shown in Fig.1c. The point (Schläfli) symbol for net is $(4^4, 6^2)$ calculated by TOPOS program and the topological type is sql.

2.2 Thermogravimetric analysis

In order to investigate the thermal stability of complexes **1**–**2**, TGA was performed in N_2 atmosphere. As shown in Fig.S3, the TGA curve of complex **1** display three weight loss steps. The first weight loss from 480 to 590 $^{\circ}C$ is attributed to the loss of one formic acid ion (Obsd. 6.7%, Calcd. 6.3%). The second weight loss of **1** between 600 and 860 $^{\circ}C$ perhaps results from the release of coordinated 1,10-Phenanthroline molecule (Obsd. 26.5%, Calcd. 25.9%). Upon heating, the framework decomposed at above 900 $^{\circ}C$. For the complex **2**, the data display the first weight loss platform at above 500 $^{\circ}C$, corresponding to the release of one formic acid ion (Obsd. 6.5%, Calcd. 6.2%). Upon temperature increase, the structure began to collapse slowly.

2.3 Luminescent properties

The luminescent properties of **1** and **2** in the solid state were investigated at room temperature. As shown in Fig.2, complex **1** exhibits maximal emission peaks at 606 nm ($\lambda_{ex}=495$ nm), suggesting that **1** may be a good visible light-emitting material. The photoluminescent mechanism is tentatively attributed to ligand-to-ligand transitions, being in reasonable agreement with this kind of metal complexes.

The fluorescence spectrum of **2** was evaluated in

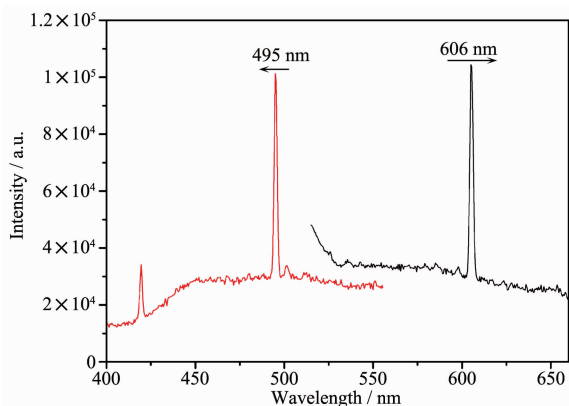


Fig.2 Solid state emission spectrum of **1**

the solid state upon the excitation at 395.5 nm at room temperature showing the $^5D_0 \rightarrow ^7F_0$ ($J=0 \sim 4$) characteristic transitions of $Eu(III)$. The strongest narrow-band emission at 615.5 nm is characteristic of the hypersensitive $^5D_0 \rightarrow ^7F_1$ transition of $Eu(III)$, which is more intense than the $^5D_0 \rightarrow ^7F_0$ transition at 591 nm, $^5D_0 \rightarrow ^7F_3$ transition at 688 nm and $^5D_0 \rightarrow ^7F_4$ transition at 697 nm. One weak emission bands at 649 nm correspond to $^5D_0 \rightarrow ^7F_2$ transitions (Fig.3). Intense red fluorescence for **2** is observed under UV excitation, suggesting that it has potential application in photoactive materials.

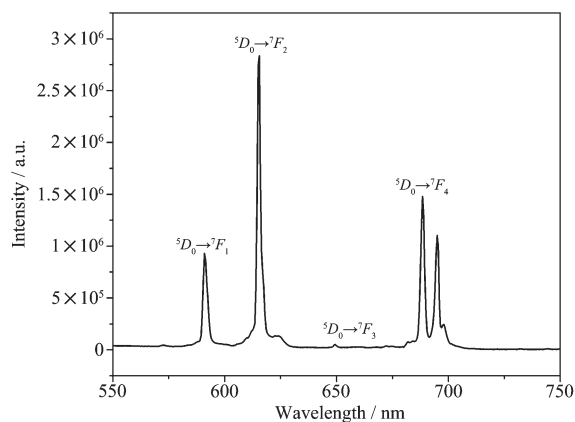


Fig.3 Solid state emission spectrum of **2**

2.4 Circular dichroism (CD) analysis

According to the $P2_12_12_1$ space group of complexes **1** and **2** and a chirality of H_2nbpd ligand (Fig.4), the study on the chirality of complexes **1** and **2** is conducted, respectively. As shown in Fig.5 ~6, compared with H_2nbpd , complexes **1** and **2** have

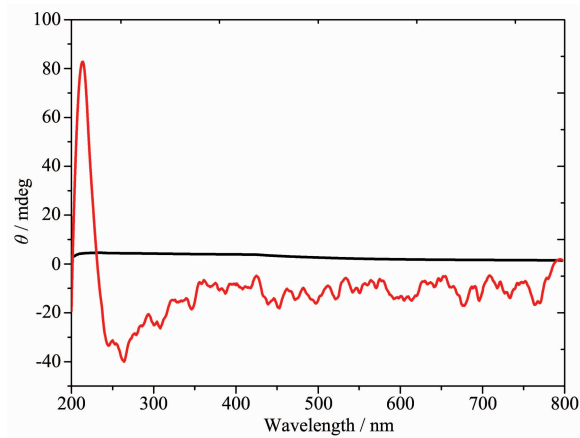


Fig.4 Circular dichroism (CD) of H_2nbpd ligand using KBr pellets at room temperature

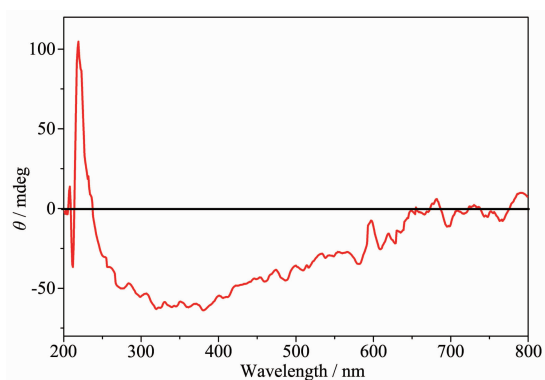


Fig.5 Circular Dichroism (CD) of complex **1** using KBr pellets at room temperature

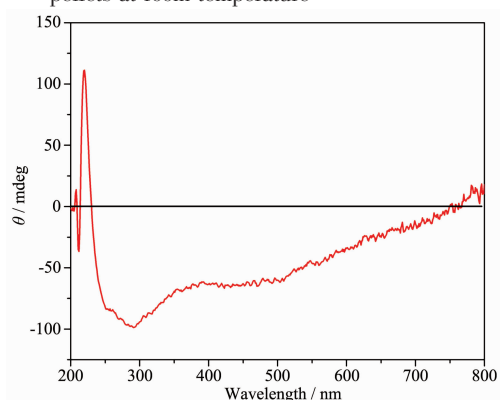


Fig.6 Circular dichroism (CD) of complex **2** using KBr pellets at room temperature

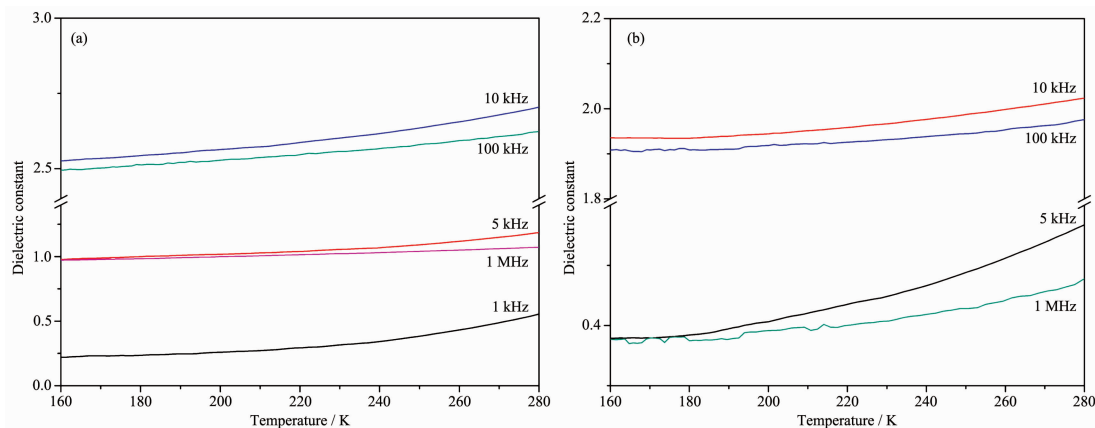


Fig.7 Dielectric constants of complexes **1** (a) and **2** (b) from 160 to 280 K at different frequencies

3 Conclusions

Two metal-organic coordination polymers based on 2,2'-dinitro-4,4'-biphenyldicarboxylic acid were successfully synthesized under hydrothermal conditions and structurally characterized. Complexes **1** and **2** generated a 3D framework with $(4^4, 6^2)$ topologies. Furthermore, complexes **1** and **2** exhibited strong

appeared correspondingly higher positive peaks at a wavelength of about 220 nm, which can be regarded as the peak of the chiral ligands. In addition, the ligand appeared wide peak at 289 nm, and compared to complexes **1** and **2**, it is expected that the peak of the complexes are similar to the peak of ligand. So it is further proved that the complexes have the chirality.

2.5 Dielectric properties

Materials with temperature-dependent dielectric constants which rapidly fluctuate may have phase transition, piezoelectric, and ferroelectric properties. The permittivities ($\epsilon = \epsilon_1 - i\epsilon_2$) of powdered samples of the two complexes as pellets were measured, where ϵ_1 and ϵ_2 are the corresponding real part and imaginary part of dielectric constant, respectively.

In addition, the dielectric constants of two complexes show similar temperature dependence (Fig. 7). The temperature-dependence dielectric constant at different frequency indicated that the dielectric constants (ϵ_1) gradually increase with a rise of temperature (160~280 K).

fluorescent emission in the solid state at room temperature.

Supporting information is available at <http://www.wjhxsb.cn>

References:

- [1] Delgado S, Sanz miguel P J, Priego J L, et al. *Inorg. Chem.*,

- 2008,47**:9128-9130
- [2] Thallapally P K, Tian J, Motkuri R K, et al. *J. Am. Chem. Soc.*, **2008,130**:16842-16843
- [3] Wang P, Ma J P, Dong Y B, et al. *J. Am. Chem. Soc.*, **2007,129**:10620-10621
- [4] Cai S L, Zheng S R, Fan J, et al. *J. Solid State Chem.*, **2011,184**:3172-3178
- [5] Hu S, He K H, Zeng M H, et al. *Inorg. Chem.*, **2008,47**:5218-5224
- [6] Eddaoudi M, Moler D B, Li H, et al. *Acc. Chem. Res.*, **2001,43**:319-330
- [7] Evans O R, Lin W. *Acc. Chem. Res.*, **2002,35**:511-522
- [8] Rosi N L, Kim J, Eddaoudi M, et al. *J. Am. Chem. Soc.*, **2005,127**:1504-1518
- [9] Chen L Z, Wang F M, Shu H. *J. Coord. Chem.*, **2012,65**:439-452
- [10] Farha O K, Hupp J T. *Acc. Chem. Res.*, **2010,43**:1166-1175
- [11] Peng R, Li M, Li D. *Coord. Chem. Rev.*, **2010,254**:1-18
- [12] Zhou H C, Long J, Yaghi O M. *Chem. Rev.*, **2012,112**:673-674
- [13] Zhao H, Qu Z R, Ye H Y, et al. *Chem. Soc. Rev.*, **2008,37**:84-100
- [14] Xu G, Guo G C, Wang M S, et al. *Angew. Chem. Int. Ed.*, **2007,46**:3249-3251
- [15] Zhang W, Xiong R G. *Chem. Rev.*, **2012,112**:1163-1195
- [16] Xu G C, Zhang W, Ma X M, et al. *J. Am. Chem. Soc.*, **2011,113**:14948-14951
- [17] CHEN Li-Zhuang(陈立庄), CAO Xing-Xing(曹星星), WANG Fang-Ming(汪芳明), et al. *Chinese J. Inorg. Chem.*(无机化学学报), **2012,28**(6):1291-1297
- [18] HUANG Deng-Deng(黄登登), CHEN Li-Zhuang(陈立庄). *Chinese J. Inorg. Chem.*(无机化学学报), **2015,31**(2):377-384
- [19] McGehee M D, Bergstedt T, Zhang C, et al. *Adv. Mater.*, **1999,11**:1349-13549
- [20] Piguet C, Bunzli J C G, Bernardinelli G, et al. *J. Am. Chem. Soc.*, **1993,115**:8197-8206
- [21] Zhao B, Chen X Y, Chen P, et al. *J. Am. Chem. Soc.*, **2004,126**:15394-15395
- [22] Sun L N, Zhang H J, Meng Q G, et al. *J. Phys. Chem. B*, **2005,109**:6174-6182
- [23] Chen L Z, Huang Y, Xiong R G, et al. *J. Mol. Struct.*, **2010,963**:16-21
- [24] Chen L Z, Huang D D. *Chin. Chem. Lett.*, **2014,25**:279-282
- [25] Chen L Z, Pan Q J, Cao X X, et al. *CrystEngComm*, **2016,18**:1944-1952
- [26] Wu R F, Zhang T L, Qiao X J. *Chin. Chem. Lett.*, **2010,21**:1007-1010
- [27] Sheldrick G M. *SHELXS-97, Program for Crystal Structure Solution*, University of Göttingen, Germany, **1997**.
- [28] Sheldrick G M. *SHELXL-97, Program for Crystal Structure Refinement*, University of Göttingen, Germany, **1997**.
- [29] Spek A L. *Acta Crystallogr. Sect. C*, **2015,C71**:9-18
- [30] Blatov V, Shevchenko A, Serezhkin V, et al. *J. Appl. Crystallogr.*, **2000,33**:1193